INTERNATIONAL SOCIETY FOR
SOIL MECHANICS AND
GEOTECHNICAL ENGINEERING

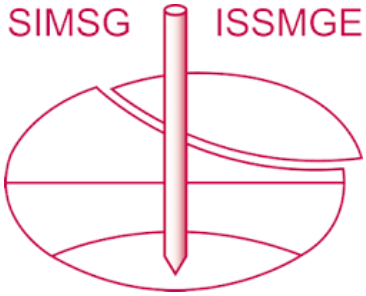

This paper was downloaded from the Online Library of the International Society for Soil Mechanics and Geotechnical Engineering (ISSMGE). The library is available here:

https://www.issmge.org/publications/online-library

This is an open-access database that archives thousands of papers published under the Auspices of the ISSMGE and maintained by the Innovation and Development Committee of ISSMGE.

The solutions of selected problems of plasticity in soil mechanics by upper-bound theorem

Les solutions de certains problèmes de plasticité en mécanique des sols

S. Škrabl, B. Macuh, H. Vrecl-Kojc, L. Trauner
University of Maribor, Faculty of Civil Engineering, Smetanova 17, 2000 Maribor, Slovenia, Email: stanislav.skrabl@uni-mb.si

ABSTRACT
The article actually presents the synthesis of the work of Institute for geotechnics on University of Maribor within last fifteen years in the field of limit state analysis. The application of the technique of the upper-bound theorem within the limit state analysis for failure load evaluation in solving stability problems of soil mechanics is presented. The solutions of the most frequent stability problems in soil mechanics that apply the upper-bound theorem within the limit analysis are presented. Different failure surfaces were introduced for two dimensional problems: polygonal for slope stability, log-spiral with polygon for bearing capacity of shallow foundation on slopes, and log-spiral and polygonal for passive pressure evaluation.

RÉSUMÉ
Cet article présente la synthèse des travaux de l'Institut de géotechnique de l'Université de Maribor dans quinze dernières années dans le domaine de l'analyse de l'état limite. L'application de la technique du théorème de la limite supérieure chez l'analyse de l'état limite pour l'évaluation de la rupture sous chargement pour résoudre des problèmes de stabilité en cadre de la mécanique des sols est présenté. Les solutions des problèmes les plus fréquents de stabilité en cadre de la mécanique des sols qui utilisent le théorème de la limite supérieure chez l'analyse limite sont démontrés. Les différentes surfaces de rupture ont été introduites pour les problèmes bi-dimensionels: une surface polygonale pour la stabilité de la pente, une surface log-spirale avec un polygone pour la capacité portante des fondations creuses sur les pentes, et une surface log-spirale et polygonale pour evaluation de la butée du sol.

Keywords : plasticity, limit analysis, upper-bound theorem, failure surface, earth pressure, stability analysis.

1 INTRODUCTION

In geotechnical practice, the results of three-dimensional analyses of passive earth pressures are used to design some anchor systems, to ensure the stability of the foundations of arching and bridging structures, to design embedded caissons and other retaining structures with spaced out vertical supporting elements, etc.

It is only logical that research into passive earth pressures is frequently presented in the literature. The major part of the research deals with 2D stability analyses, while much less attention is paid to 3D analyses. The magnitudes of the earth pressures for the active and passive limit states can be determined by different methods: the limit-equilibrium method (Terzaghi 1943), the slip-line method (Sokolovski 1965) and the limit-analysis method (Chen 1975). In the limit-equilibrium and slip-line methods the static equilibrium and failure conditions are considered, while the expected movements of the retaining structures are not directly considered in the analysis. Generally, a limit analysis serves for determining the upper and lower bounds of the true collapse load by taking into account the supposed movements. The results of the analyses can differ essentially, because they depend on the chosen failure mechanism or the kinematic model of the limit state. Irrespective of the chosen procedure and the method used, the considered static or kinematic model should be in equilibrium when the limit state is reached.

Researchers have used many different methods to determine earth pressures, among them Coulomb (1776), Brinch Hansen (1953), Janbu (1957), Lee and Herington (1972), Shields and Tolunay (1973), Kérisel and Absi (1990), Kumar and Subba Rao (1997), Soubra and Regenass (2000), Soubra (2000), Škrabl and Macuh (2005) and Vrecl-Kojc and Škrabl (2007).

The above-cited, published research mainly considers the 2D problem of passive earth pressures. The results of 3D analyses have been presented only by Blum (1932), and to a restricted extent. Extensive 3D analyses were treated by Ovesen (1964), who presented the procedure for determining the bearing capacity of different anchor plates based on 2D solutions of passive earth pressures and the results of several experimental studies in 3D conditions.

Soubra and Regenass (2000) published the results of an analysis for determining the 3D passive pressure according to the limit-state analysis using the upper-bound theorem for the translator kinematic admissible multi-block failure mechanism. Duncan and Mokwa (2001) treated the procedures for determining the bearing capacities for anchor plates and presented the results of several experimental studies. Škrabl and Macuh (2005) presented the procedure for a spatial passive pressure analysis based on the hyperbolic kinematic admissible failure mechanism and the upper-bound theorem.

2 ASSUMPTIONS AND LIMITATIONS

It is characteristic for passive earth pressures under 3D conditions to increase, essentially with reduction of the wall width. The value depends on the ground properties and the height/width relationship of the wall. It can be several times higher than the value for 2D cases. The presented analysis is based on the following suppositions and limitations:

- the structure discussed is a vertical wall with an area of b×h (b = width; h = height) and a horizontal backfill
- the resulting value of passive earth pressure is defined by:

$$P_p = K_{p\gamma} \cdot \gamma \frac{h^2}{2} b + K_{pc} \cdot c \cdot h \cdot b + K_{pq} \cdot q \cdot h \cdot b \quad (1)$$

Proceedings of the 17th International Conference on Soil Mechanics and Geotechnical Engineering
M. Hamza et al. (Eds.)
© 2009 IOS Press.
doi:10.3233/978-1-60750-031-5-1449

- the redistribution of contact pressures over the wall height for that part of passive earth pressures due to soil weight (g) is triangular, while it is uniform for the parts due to cohesive strength (c) and surcharge loading (q)
- the discussed rotational failure mechanism is bounded by the log-spiral in the region of the retaining wall, and by the hyperbolic surfaces defined by the envelope of the connected hyperbolic half-cones at the lateral sides
- the lateral surfaces coincide with the margins of the considered retaining wall
- the rate of work due to external forces, induced by passive earth pressures, is determined by considering the assumed redistribution of contact pressures over the wall height
- the backfill is homogenous, the soil is isotropic and considered as a Coulomb material with the associative flow rule obeying Hill's maximal work principle
- it is assumed that the backfill soil fulfills the Mohr-Coulomb plastification criteria with the associative plastic flow rule. The change of energy dissipation per volume unit of backfill soil can be evaluated by (Michalowski, 2001):

$$\dot{D} = -\dot{\varepsilon}_v \, c \cos\phi = -(\dot{\varepsilon}_1 + \dot{\varepsilon}_3) c \cot\phi \tag{2}$$

2.1 *The upper- and lower-bound theorems*

The upper-bound theorem ensures that the rate of the work due to the external forces of the kinematic systems in equilibrium is smaller than, or equal to, the rate of dissipated internal energy for all kinematically admissible velocity fields. The kinematically admissible velocity fields obey strain-velocity compatibility conditions and velocity boundary conditions, as well as the flow rule of the considered materials. The lower-bound theorem for rigid-plastic material using the associative flow rule enables an evaluation of the lower-bound theorem of the true passive earth pressures for each statically admissible stress field that satisfies the equilibrium and stress boundary conditions, and does not violate the yield criteria anywhere. The true value of the failure load is bracketed between both limit values with the expected deviations, which are usually acceptable in geotechnical design.

3 FAILURE MECHANISMS

For calculations of passive pressures different failure mechanisms were employed, and two of them are presented.

3.1 *Translational failure mechanism – 3D*

The 3D translational failure mechanism is applied in analyses (Škrabl and Macuh, 2005). It represents an extension of the plane slip surface in the shape of a log spiral (see Fig. 1a). A very similar 'friction cone' mechanism in the upper-bound analysis of a 3D bearing capacity problem was used by Michalowski (2001). The movement with a velocity $V_1 = 1$ at point 1 is being undertaken by the wall (see Fig. 1b). The velocities and velocity hodograph in Fig. 1a demonstrate that relative motion between the soil and the wall is kinematically admissible. A failure mechanism is kinematically admissible if the corresponding shear stress on the soil-wall interface is opposing the motion of the wall relative to the adjoining wedge (Kumar and Subba Rao 1997).

The velocities exist only inside the failure mechanism. The directions of the velocities vectors are perpendicular to the radius r, their intensity is defined by (3). The soil velocities in the lateral bodies are independent of z due to no relative movement in the plane r-z.

$$V(\vartheta) = V_1 \cdot e^{(\vartheta - \vartheta_1)\tan\phi} \tag{3}$$

where V_1 denotes the velocity at the toe of the retaining structure at the point where $r = r_1$ and $\vartheta = \vartheta_1$.

The external rate of work is due to the passive earth pressures in the contact surface between the retaining structure and the ground, the soil weight of the whole failure body and the surcharge loadings. The internal rate of the system's energy dissipation is due to velocity field discontinuities inside the failure body and along the failure surface, as defined by the log-spiral segment.

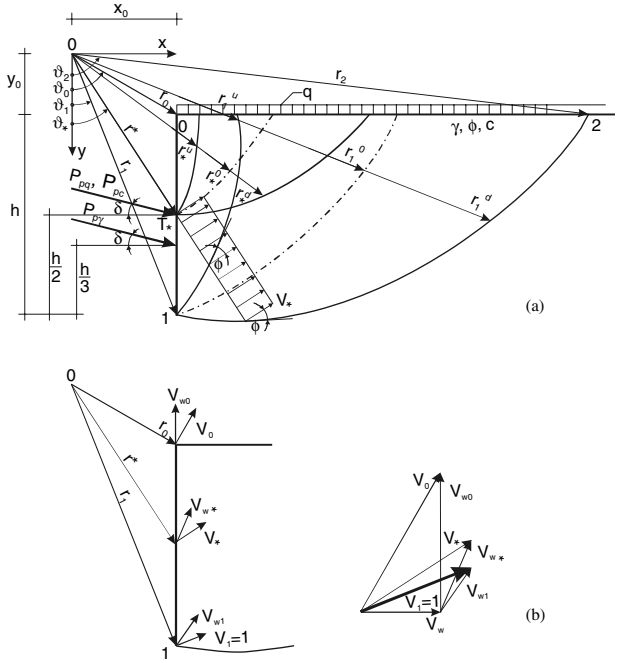

Figure 1. Notation of passive earth pressure analysis: (a) log-spiral slip surface, (b) velocities with hodograph.

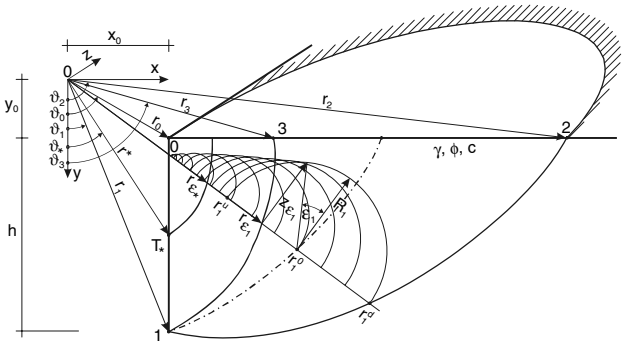

Figure 2. The scheme of the spatial failure mechanism.

3.2 *Modified translational failure mechanism – 3D*

The applied modified 3D translational failure mechanism (Škrabl, 2008) represents an extension of the plane slip surface in the shape of a log spiral (see Fig. 3). A very similar 'friction cone' mechanism in the upper-bound analysis of a 3D bearing-capacity problem was used by Michalowski (2001).

The considered failure mechanism on the width b is limited on the left by a vertical wall, on the right by a curved surface in the shape of a log spiral, and above by an even surface on which the surcharge can act. Both lateral surfaces are defined by the curved surfaces of the leading half-cone and the envelope of all the other hyperbolic half-cones (see Fig. 4).

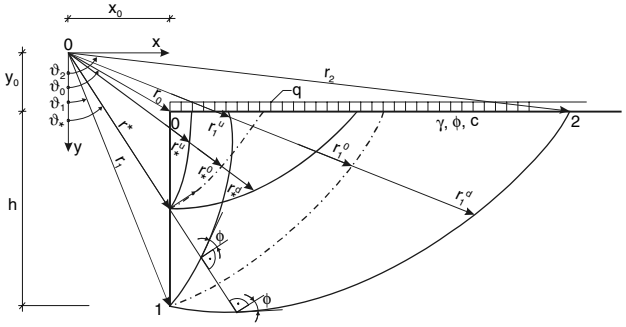

Figure 3. Cross-section of the 3D failure mechanism.

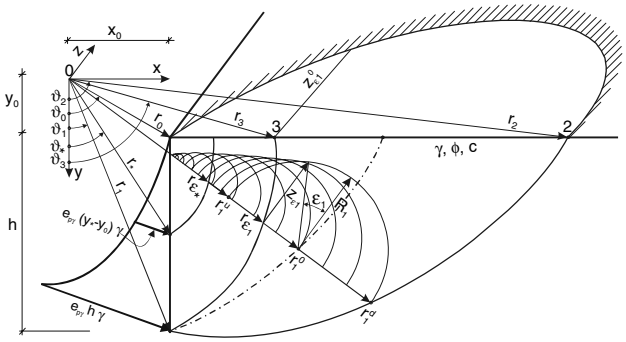

Figure 4. The scheme of the spatial failure mechanism.

At each point on the so-formed failure surface the normal vector of the surface encloses with the plane *r*-*z* shear angle ϕ and also defines the direction of the normal stress to the surface (see Fig. 5).

$$dN = \sigma\, dA, \quad dT_\phi = dN \tan\phi, \quad dQ_\phi = \sqrt{dN^2 + dT_\phi^2} \tag{4}$$

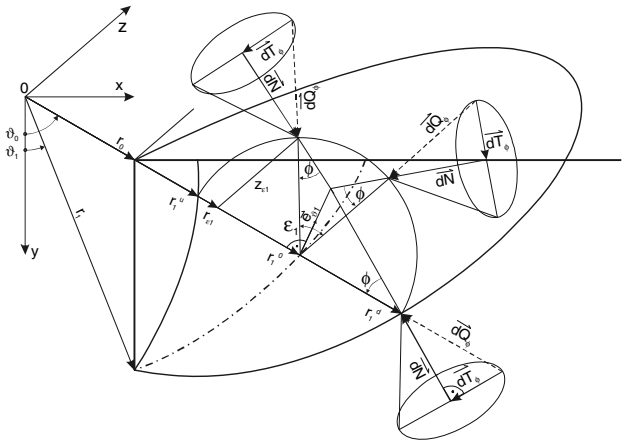

Figure 5. The forces on the failure surface.

4 WORK EQUATION

The work equation equalizes the external rate of work and the internal rate of energy dissipation along the velocity field's discontinuities and ensures the energy balance of the kinematical system in the limit state.

The external rate of work is caused by the resultant force of passive earth pressures P_p, unit weight of the backfill soil γ and surcharge loading on the backfill surface q.

$$\dot{W} = \dot{W}_{P_p} + \dot{W}_\gamma + \dot{W}_q \tag{5}$$

The internal rate of dissipation of the analyzed failure mechanism is only due to the cohesion strength of the soil c along the velocity field's discontinuities on the surfaces between the resting and the moving parts of the backfill soil, and inside the failure body:

$$\dot{D} = \dot{D}_c \tag{6}$$

5 RESULTS

5.1 *Translational failure mechanism – 3D*

Mathematical optimization was used to determine the unknown parameters ϑ_1 and ϑ_2 of the critical failure surface.

Fig. 6 presents the ground plan and a cross-section of the hyperbolic failure mechanism in the x0y plane, determined by minimization of the $K_{p\gamma}$ coefficient. Fig.6a shows the shape of the failure mechanism when there is no friction between the soil and wall $\delta/\phi = 0$, while Fig. 6b presents the failure mechanism for fully mobilized friction between the soil and wall $\delta/\phi = 1$.

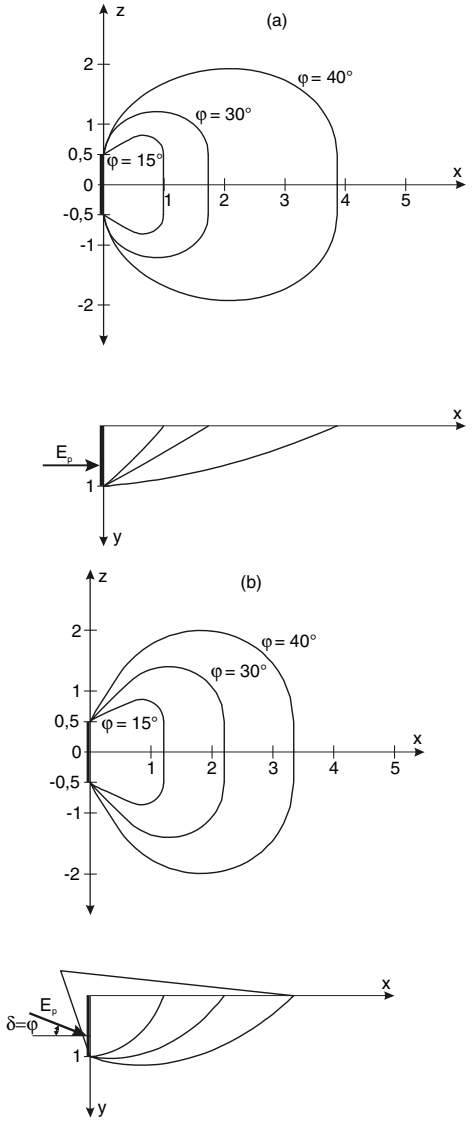

Figure 6. Ground plan and cross-section of the hyperbolic failure mechanism: (a) $\delta/\phi = 0$, $b/h = 1$, $\phi = 15°, 30°, 40°$; (b) $\delta/\phi = 1$, $b/h = 1$, $\phi = 15°, 30°, 40°$.

5.2 *Modified translational failure mechanism – 3D*

Mathematical optimization was used to determine the unknown parameters ϑ_1 and ϑ_2 of the critical failure surface, which defines, in the considered calculation step, the minimal value of the unknown factor of the passive pressure distribution, $e^m_{p\gamma}$ and e^m_{pq}, at the toe of the wall.

The Solver Optimization Tool (Microsoft Excel) with the generalized-reduced-gradient method was used in the minimization process.

The result of the gradual determination of the passive pressure distribution factors from the top of the wall downwards are the numerical values of the factors $e_{p\gamma}$ and e_{pq}, and a set of spatial failure surfaces that are presented in Fig. 7 for the case when $\phi = 40°$ and $\delta/\phi = 1$.

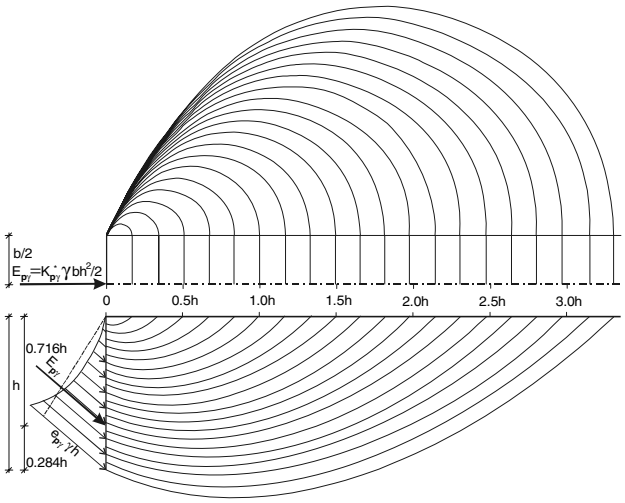

Figure 7. Set of spatial failure surfaces.

The values of the comparative passive pressure coefficients, $K^*_{p\gamma}$ and K^*_{pq}, and the distances of the handling points of the resultants, a_γ, and a_q, from the surface of the backfill soil are also part of results.

6 CONCLUSIONS

The presented procedures are applicable for the determination of earth pressures on embedded retaining structures: pile walls, caissons, foundations of the columns of bridging structures, etc; bearing capacity of shallow foundation and stability analysis of slopes.

The solutions for given problems in soil mechanics using the upper-bound theorem of the limit analysis are clear and uniquely defined conceptually. The considered approach does not require any additional assumptions and simplifications due to the statically undetermined problem, which are typically required for the limit equilibrium method.

The advantage of the upper-bound approach is in the clearness of the calculation concept and the simple supplements needed for the generalization of the solution for the cases of slopes, non-homogenous ground, and the presence of seepage forces.

The results of the numerical analyses indicate that, when considering the upper-bound theorem and the set of three-dimensional kinematically admissible hyperbolic translational failure mechanisms, the passive-earth-pressure coefficients are lower than in the case of the hyperbolic translational failure mechanism and the translational mechanisms published in the literature for $b/h < 10$. The upper-bound values of the comparative passive-earth-pressure coefficients with a calculated pressure distribution are lower than the existing solutions with an assumed pressure distribution obtained using the upper-bound method within the framework of the limit analysis. This means that the classically presumed passive-earth-pressure distribution in 3D analyses is not acceptable, because it can actually not be activated. Furthermore, the trust point of the passive pressures resultant is independent of the friction between the retaining structures and the soil.

The upper-bound values of the passive earth pressure coefficients are generally lower than existing solutions obtained using the upper-bound method within the framework of limit analysis. Therefore the presented results are applicable in geotechnical practice.

REFERENCES

Blum, H. 1932. Wirtschaftliche Dalbenformen und deren Berechnung. *Bautechnik*, 10(5): 122-135 (in German).

Brinch Hansen, J. (1953). *Earth Pressure Calculation*, Danish Technical Press, Copenhagen.

Chen, W. F. 1975. *Limit analysis and soil plasticity*. Elsevier Scientific Publishing Company, Amsterdam, The Netherlands.

Coulomb, C. A. 1776. Essai sur une application des règles de maximis et minimis à quelques problèmes de statique relatifs à l'architecture. *Mémoire présenté à l'académie Royale des Sciences, Paris*, Vol. 7, 343-382 (in French).

Duncan, J. M. & Mokwa, R. L. 2001. Passive earth pressures: Theories and tests. *Journal of Geotechnical and Geoenvironmental Engineering Division*, ASCE, 127(3): 248-257.

Janbu, N. 1957. Earth pressure and bearing capacity calculations by generalised procedure of slices. *In Proceedings of the 4th International Conference*, International Society of Soil Mechanics and Foundation Engineering: 207-213.

Lee, I. K. & Herington, J. R. 1972. A theoretical study of the pressures acting on a rigid wall by a sloping earth on rockfill. *Géotechnique*, London, 22(1): 1-26.

Kérisel, J. & Absi, E. 1990. *Tables for the calculation of passive pressure, active pressure and bearing capacity of foundations*. Gauthier-Villard, Paris, France.

Kumar, J. & Subba Rao, K. S. 1997. Passive pressure coefficients, critical failure surface and its kinematic admissibility. *Géotechnique*, London, England, 47(1): 185-192.

Michalowski, R. L. 2001. Upper-bound load estimates on square and rectangular footings. *Géotechnique*, The Institution of Civil Engineering, London, England, 51(9): 787-798.

Mroz, Z. & Drescher, A. 1969. Limit plasticity approach to some cases of flow of bulk solids. *Journal of Engineering for Industry, Transactions of the ASME*, 91: 357-364.

Ovesen, N. K. 1964. Anchor slabs, calculation methods, and model tests. *Bull. No. 16*, Danish Geotechnical Institute, Copenhagen: 5-39.

Salençon, J. 1990. An introduction to the yield design theory and its applications to soil mechanics. *European Journal of Mechanics – A/Solids, Paris*, 9(5): 477-500.

Shields, D. H. & Tolunay, A. Z. 1973. Passive pressure coefficients by method of slices. *Journal of the Soil Mechanics and Foundation Division*, ASCE, 99(12): 1043-1053.

Škrabl, S. 2008. The limit values and the distribution of three-dimensional passive earth pressures. *Acta Geotechnica Slovenica*, 5(1): 20-34.

Škrabl, S. & Macuh, B. 2005. Upper-bound solutions of three-dimensional passive earth pressures. *Canadian Geotechnical Journal*, Ottawa, 42: 1449-1460.

Sokolovski, V. V. 1965. *Static of granular media*. Pergamon Press, New York.

Soubra, A. H. 2000. Static and seismic earth pressure coefficients on rigid retaining structures. *Canadian Geotechnical Journal*, Ottawa, 37: 463-478.

Soubra, A. H., & Regenass, P. 2000. Three-dimensional passive earth pressure by kinematical approach. *Journal of Geotechnical and Geoenvironmental Engineering Division*, ASCE, 126(11): 969-978.

Terzaghi, K. (1943). *Theoretical soil mechanics*. Wiley, New York.

Vrecl-Kojc, H. & Škrabl, S. 2007. Determination of passive earth pressure using three-dimensional failure mechanism. *Acta Geotechnica Slovenica*, 4(1): 10-23.